Results in Physics 25 (2021) 104235

Contents lists available at ScienceDirect

Results in Physics

journal homepage: www.elsevier.com/locate/rinp

A novel study of Morlet neural networks to solve the nonlinear HIV infection system of latently infected cells

Muhammad Umar [a], Zulqurnain Sabir [a], Muhammad Asif Zahoor Raja [b], Haci Mehmet Baskonus [c], Shao-Wen Yao [d,*], Esin Ilhan [e]

[a] Department of Mathematics and Statistics, Hazara University, Mansehra, Pakistan
[b] Future Technology Research Center, National Yunlin University of Science and Technology, 123 University Road, Section 3, Douliou, Yunlin 64002, Taiwan, ROC
[c] Department of Mathematics and Science Education Harran University, Sanliurfa, Turkey
[d] School of Mathematics and Information Science, Henan Polytechnic University, Jiaozuo 454000, China
[e] Kirsehir Ahi Evran University, Kirsehir, Turkey

ARTICLE INFO

Keywords:
Morlet wavelets
HIV infection models
Genetic algorithms
Neural networks
Sequential quadratic programming
Bioinformatics

ABSTRACT

The aim of this study is to provide the numerical outcomes of a nonlinear HIV infection system of latently infected CD4+ T cells exists in bioinformatics using Morlet wavelet (MW) artificial neural networks (ANNs) optimized initially with global search of genetic algorithms (GAs) hybridized for speedy local search of sequential quadratic programming (SQP), i.e., MW-ANN-GA-SQP. The design of an error function is presented by designing the MW-ANN models for the differential equations along with the initial conditions that represent the HIV infection system involving latently infected CD4+ T cells. The precision and persistence of the presented approach MW-ANN-GA-SQP are recognized through comparative studies from the results of the Runge-Kutta numerical scheme for solving the HIV infection spread system in case of single and multiple trails of the MW-ANN-GA-SQP. Statistical estimates with 'Theil's inequality coefficient' and 'root mean square error' based indices further validate the sustainability and applicability of proposed MW-ANN-GA-SQP solver.

Introduction

There are many dangers, hazardous and harmful viruses, one of them is HIV virus that causes to manipulate the body fluids and destroy the immune system. The affected body from HIV virus fails to fight against infections and diseases, because HIV kills several CD4 or T-cells. The body's performance to fight against diseases, illnesses and infections gets weak when the immune system of the body gets disturbed. Many global, serious diseases like AIDS/HIV, cancer and adaptable infections create the weak body's advantage due to the immune system. For these dangerous diseases and harmful viruses, extensive efforts in order to increase the complexity of SIRS models, but still no treatment is discovered [1].Several researchers have tried to present many valuable mathematical designs to understand the HIV infection dynamics [2–6]. They showed that latently T-cells are provoked due to the occurrence of HIV virus and designed an HIV infection spread mathematical model in 1989 [7]. The main topographies of this mathematical model have three terms: infected rate, uninfected rate (UR) and free from virus cells.

Some HIV systems increased the complexity by incorporating the SIR model, where the diseased CD4+ T-cells are presumed to present the HIV infection [8]. A large number of strong T-cells lost because of the infection; however, a few T-cells may be infected productively, i.e., the state of latent or active. The most simplistic method of modeling HIV infection along with the initial values (IVs) is given as [9,10]:

$$\begin{cases} X'(t) = \mu - dX - \alpha XV, & X_0 = I_1, \\ W'(t) = -(q-1)\alpha XV - eW - \lambda W, & W_0 = I_2, \\ Y'(t) = \lambda W - aY + q\alpha XV, & Y_0 = I_3, \\ V'(t) = -V + kY, & V_0 = I_4. \end{cases} \tag{1}$$

where X, W, Y, and V used for susceptible virus, infected virus, recover virus and latently infected virus of CD4+ T cells, respectively. I_1, I_2, I_3 and $I_4$are the respective initial conditions, α denotes the infection rate, λ is a constant indicate the recovery rate, μ stands the UR of CD4+ T cells, d shows the death ratio for susceptible CD4+ T cells, a denotes the death ratio of HIV improve cells, e is used for infection rate, k is called latently rate of infection of HIV cells and q is the elimination rate. To present the solution of the nonlinear biological HIV infection model of

* Corresponding author.
E-mail address: yaoshaowen@hpu.edu.cn (S.-W. Yao).

https://doi.org/10.1016/j.rinp.2021.104235
Received 15 February 2021; Received in revised form 21 April 2021; Accepted 22 April 2021
Available online 1 May 2021

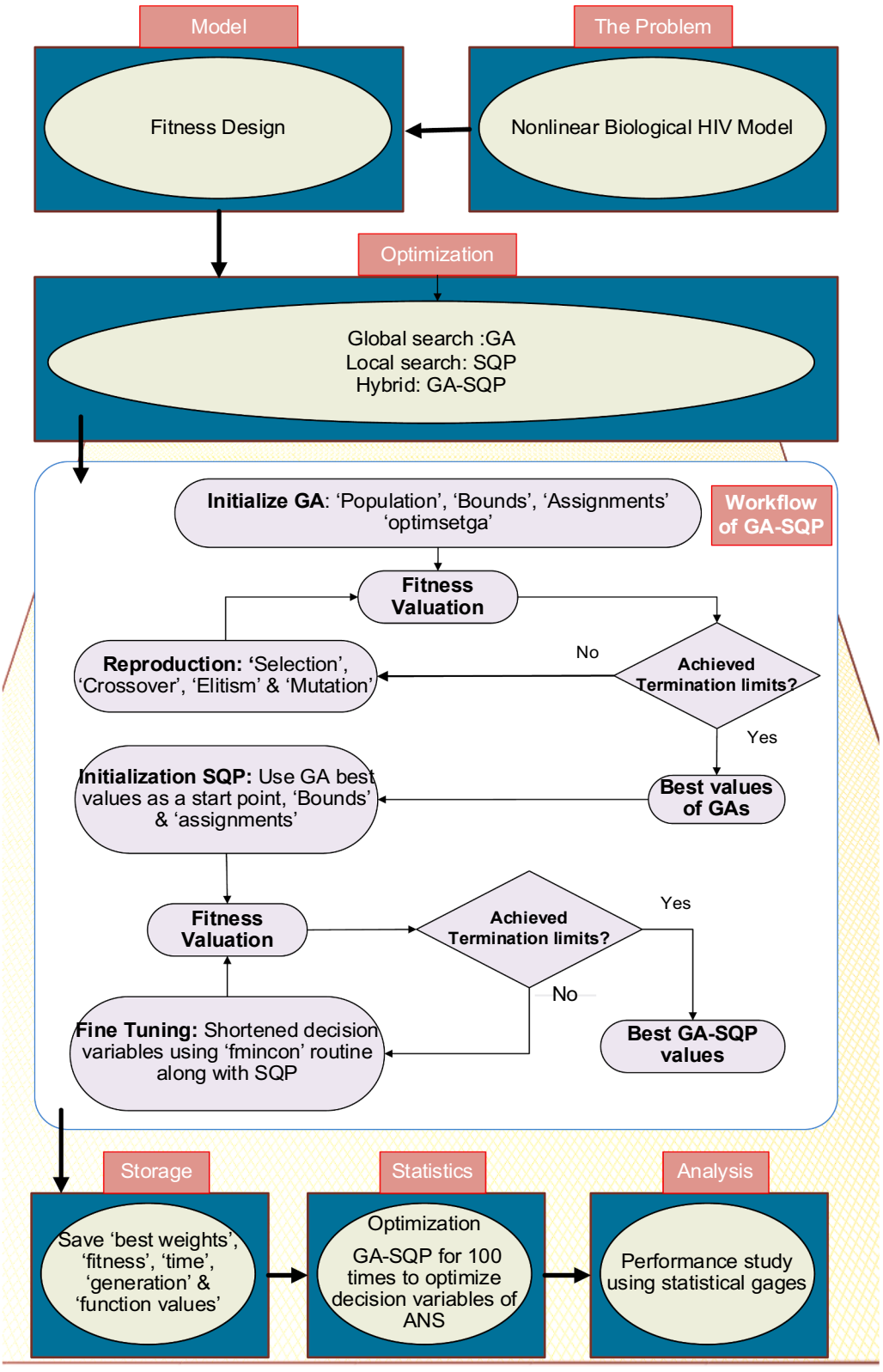

Fig. 1. Graphical representations of proposed designed technique for HIV biological model of latently infected T-cells.

latently infected CD4+ T cells given in equation (1), only a few existing schemes is available in the literature. Some of them are finite difference method [11], sequential Bayesian analysis technique [12], Legendre wavelet approach [13], a homotopy analysis scheme [14], the Bessel collocation approach [15] and approach based on differential transformation [16].

All the above-stated methods have their separate advantages/disadvantages, merits/demerits, while, the solvers based on the artificial neural systems (ANN) are found to be precise, efficient and reliable to handle optimization models arising in numerous fields [17–21]. Recently, some worthy applications of stochastic numerical solvers are nonlinear prey-predator models [22],spreading infection and treatment

[23],singular systems represented with second kind nonlinear Lane-Emden model [24–25], thermal analysis of porous fin model [26],fractional Meyer wavelet neural networks[27–28],singular functional differential model [29–30], nano fluidic models [31], nonlinear Thomas-Fermi models [32], doubly-singular model [33], conduction of heat in the human head model [34], and nonlinear multi-singular third order model [35].Keeping in view these well-established applications in different fields, the authors are motivated to investigate the intelligent computing to design an alternate framework by exploiting the modeling ability of Morlet Wavelet (MW) artificial neural networks (ANN) optimized with genetic algorithms (GAs) enhanced with rapid sequential quadratic programming (SQP), i.e., MW-ANN-GA-SQP scheme for solving the HIV infection spread model.

Some innovative contribution of proposed MW-ANN-GA-SQP solver are listed as follows:

- A novel development of MW-ANN is presented to design an alternate, accurate, consistent and stable computational intelligent numerical solver for nonlinear biological HIV infection system of latently infected CD4+ T cells.
- The solution of the nonlinear biological HIV infection system of latently infected CD4+ T cells is presented effectively by exploiting the strength of MW-ANN modeling and combined optimization capability of GAs-SQP.
- The worth of the proposed MW-ANN-GA-SQP solver is certified with overlapping solutions of Runge-Kutta up to 5 to 7 decimal level of accuracy.
- Validation through statistical enlightenments based on different performance indices for measures of central tendency and dispersion in terms of minimum, standard deviation, maximum and median.

The other parts of this work are systematized as: Section 2 expresses the designed methodology using the MW-ANNs along with performance indices, Section 4 presents the detailed result and discussions. The conclusion is drawn in the final Section.

Design procedure

The designed arrangement of the MW-ANN to solve the HIV system given in Eq. (1) is provided in this section. The construction of fitness function using the MW-ANN along with the optimization of the GA-SQP is presented. Moreover, the graphical plots of GA-SQP is given in Fig. 1.

2.1Modeled form of the MW-ANN

The mathematical procedures of the HIV system (1) are represented with feed-forward ANN in the form of proposed solutions$\widehat{X}(t)$, $\widehat{W}(t)$, $\widehat{Y}(t)$ and $\widehat{V}(t)$ along with the nth derivatives are written as:

$$\begin{bmatrix} \widehat{X}(t), \widehat{W}(t), \\ \widehat{Y}(t), \widehat{V}(t) \end{bmatrix} = \begin{bmatrix} \sum_{i=1}^{m} \phi_{X,i} g(\rho_{X,i} t + b_{X,i}), & \sum_{i=1}^{m} \phi_{W,i} g(\rho_{W,i} t + b_{W,i}), \\ \sum_{i=1}^{m} \phi_{Y,i} g(\rho_{Y,i} t + b_{Y,i}), & \sum_{i=1}^{m} \phi_{V,i} g(\rho_{V,i} t + b_{V,i}) \end{bmatrix}, \tag{2}$$

$$\begin{bmatrix} \widehat{X}^{(n)}, \widehat{W}^{(n)}, \\ \widehat{Y}^{(n)}, \widehat{V}^{(n)} \end{bmatrix} = \begin{bmatrix} \sum_{i=1}^{m} \phi_{X,i} g^{(n)}(\rho_{X,i} t + b_{X,i}), & \sum_{i=1}^{m} \phi_{W,i} g^{(n)}(\rho_{W,i} t + b_{W,i}), \\ \sum_{i=1}^{m} \phi_{Y,i} g^{(n)}(\rho_{Y,i} t + b_{Y,i}), & \sum_{i=1}^{m} \phi_{V,i} g^{(n)}(\rho_{V,i} t + b_{V,i}) \end{bmatrix}$$

Where $\boldsymbol{W}$ denotes the unidentified weight vector, given as: $\boldsymbol{W} = [\boldsymbol{W}_X, \boldsymbol{W}_W, \boldsymbol{W}_Y, \boldsymbol{W}_V]$, for$\boldsymbol{W}_X = [\boldsymbol{\phi}_X, \boldsymbol{\rho}_X, \boldsymbol{b}_X]$,$\boldsymbol{W}_W = [\boldsymbol{\phi}_W, \boldsymbol{\rho}_W, \boldsymbol{b}_W]$$\boldsymbol{W}_Y = [\boldsymbol{\phi}_Y, \boldsymbol{\rho}_Y, \boldsymbol{b}_Y]$ and $\boldsymbol{W}_V = [\boldsymbol{\phi}_V, \boldsymbol{\rho}_V, \boldsymbol{b}_V]$. where

MW-ANN has never been used for solving the HIV model. The MW activation function is written as [36]:

$$\boldsymbol{\phi}_X = [\phi_{X,1}, \phi_{X,2}, ..., \phi_{X,m}], \quad \boldsymbol{\phi}_W = [\phi_{W,1}, \phi_{W,2}, ..., \phi_{W,m}], \quad \boldsymbol{\phi}_Y = [\phi_{Y,1}, \phi_{Y,2}, ..., \phi_{Y,m}], \quad \boldsymbol{\phi}_V = [\phi_{V,1}, \phi_{V,2}, ..., \phi_{V,m}],$$
$$\boldsymbol{\rho}_X = [\rho_{X,1}, \rho_{X,2}, ..., \rho_{X,m}], \boldsymbol{\rho}_W = [\rho_{W,1}, \rho_{W,2}, ..., \rho_{W,m}], \boldsymbol{\rho}_Y = [\rho_{Y,1}, \rho_{Y,2}, ..., \rho_{Y,m}], \boldsymbol{\rho}_V = [\rho_{V,1}, \rho_{V,2}, ..., \rho_{V,m}],$$
$$\boldsymbol{b}_X = [b_{X,1}, b_{X,2}, ..., b_{X,m}], \quad \boldsymbol{b}_W = [b_{W,1}, b_{W,2}, ..., b_{W,m}], \quad \boldsymbol{b}_Y = [b_{Y,1}, b_{Y,2}, ..., b_{Y,m}], \boldsymbol{b}_V = [b_{V,1}, b_{V,2}, b_{V,3}, ..., b_{V,m}].$$

$$g(t) = (cos(1.75t))^{*}\left(exp\left(-0.5t^2\right)\right) \tag{3}$$

Using Eq. (3), the updated form of system (2) is converted as:

$$\begin{bmatrix} \widehat{X}(t), \widehat{W}(t), \\ \widehat{Y}(t), \widehat{V}(t) \end{bmatrix} = \begin{bmatrix} \sum_{i=1}^{m} \phi_{X,i} cos[1.75(\rho_{X,i} t + b_{X,i})] \times e^{-0.5(\rho_{X,i} t + b_{X,i})^2}, \\ \sum_{i=1}^{m} \phi_{W,i} cos[1.75(\rho_{W,i} t + b_{W,i})] \times e^{-0.5(\rho_{W,i} t + b_{W,i})^2}, \\ \sum_{i=1}^{m} \phi_{Y,i} cos[1.75(\rho_{Y,i} t + b_{Y,i})] \times e^{-0.5(\rho_{Y,i} t + b_{Y,i})^2}, \\ \sum_{i=1}^{m} \phi_{V,i} cos[1.75(\rho_{V,i} t + b_{V,i})] \times e^{-0.5(\rho_{V,i} t + b_{V,i})^2} \end{bmatrix},$$

$$\begin{bmatrix} \widehat{X}'(t), \widehat{W}'(t), \\ \widehat{Y}'(t), \widehat{V}'(t) \end{bmatrix} = \begin{bmatrix} \sum_{i=1}^{m} -\phi_{X,i}\rho_{X,i} e^{\left(-0.5(\rho_{X,i} t + b_{X,i})^2\right)} \left(\begin{matrix} sin\{1.75(\rho_{X,i} t + b_{X,i})\} + \\ (\rho_{X,i} t + b_{X,i}) cos\{1.75(\rho_{X,i} t + b_{X,i})\} \end{matrix} \right), \\ \sum_{i=1}^{m} -\phi_{W,i}\rho_{W,i} e^{\left(-0.5(\rho_{W,i} t + b_{W,i})^2\right)} \left(\begin{matrix} sin\{1.75(\rho_{W,i} t + b_{W,i})\} + \\ (\rho_{W,i} t + b_{W,i}) cos\{1.75(\rho_{W,i} t + b_{W,i})\} \end{matrix} \right), \\ \sum_{i=1}^{m} -\phi_{Y,i}\rho_{Y,i} e^{\left(-0.5(\rho_{Y,i} t + b_{Y,i})^2\right)} \left(\begin{matrix} sin\{1.75(\rho_{Y,i} t + b_{Y,i})\} + \\ (\rho_{Y,i} t + b_{Y,i}) cos\{1.75(\rho_{Y,i} t + b_{Y,i})\} \end{matrix} \right), \\ \sum_{i=1}^{m} -\phi_{V,i}\rho_{V,i} e^{\left(-0.5(\rho_{V,i} t + b_{V,i})^2\right)} \left(\begin{matrix} sin\{1.75(\rho_{V,i} t + b_{V,i})\} + \\ (\rho_{V,i} t + b_{V,i}) cos\{1.75(\rho_{V,i} t + b_{V,i})\} \end{matrix} \right) \end{bmatrix} \tag{4}$$

Table 1
Pseudo code using MW-ANN-GA-SQP.

Start of GA
Inputs:
"The chromosome having equal entries of the network"
$\boldsymbol{W} = [\boldsymbol{W}_X, \boldsymbol{W}_W, \boldsymbol{W}_Y, \boldsymbol{W}_V]$, $\boldsymbol{W}_X = [\boldsymbol{\phi}_X, \boldsymbol{\rho}_X, \boldsymbol{b}_X]$, $\boldsymbol{W}_W = [\boldsymbol{\phi}_W, \boldsymbol{\rho}_W, \boldsymbol{b}_W]$, $\boldsymbol{W}_Y = [\boldsymbol{\phi}_Y, \boldsymbol{\rho}_Y, \boldsymbol{b}_Y]$ and $\boldsymbol{W}_V = [\boldsymbol{\phi}_V, \boldsymbol{\rho}_V, \boldsymbol{b}_V]$. where

$\boldsymbol{\phi}_X = [\phi_{X,1}, \phi_{X,2}, ..., \phi_{X,m}]$, $\boldsymbol{\phi}_W = [\phi_{W,1}; \phi_{W,2}; ..., \phi_{W,m}]$,
$\boldsymbol{\phi}_Y = [\phi_{Y,1}, \phi_{Y,2}, ..., \phi_{Y,m}]$, $\boldsymbol{\phi}_V = [\phi_{V,1}, \phi_{V,2}, ..., \phi_{V,m}]$,
$\boldsymbol{\rho}_X = [\rho_{X,1}, \rho_{X,2}, ..., \rho_{X,m}]$, $\boldsymbol{\rho}_W = [\rho_{W,1}; \rho_{W,2}, ..., \rho_{W,m}]$,
$\boldsymbol{\rho}_Y = [\rho_{Y,1}, \rho_{Y,2}, ..., \rho_{Y,m}]$, $\boldsymbol{\rho}_V = [\rho_{V,1}, \rho_{V,2}, ..., \rho_{V,m}]$,
$\boldsymbol{b}_X = [b_{X,1}, b_{X,2}, ..., b_{X,m}]$, $\boldsymbol{b}_W = [b_{W,1}, b_{W,2}, ..., b_{W,m}]$,
$\boldsymbol{b}_Y = [b_{Y,1}, b_{Y,2}, ..., b_{Y,m}]$, $\boldsymbol{b}_V = [b_{V,1}, b_{V,2}, b_{V,3}, ..., b_{V,m}]$.

Population: The chromosomes set is
$\boldsymbol{P} = [(\boldsymbol{W}_{X1}, \boldsymbol{W}_{X2}, ..., \boldsymbol{W}_{Xn}), (\boldsymbol{W}_{W1}, \boldsymbol{W}_{W2}, ..., \boldsymbol{W}_{Wn}), (\boldsymbol{W}_{Y1}, \boldsymbol{W}_{Y2}, ..., \boldsymbol{W}_{Yn}), (\boldsymbol{W}_{V1}, \boldsymbol{W}_{V2}, ..., \boldsymbol{W}_{Vn})]$
$[\boldsymbol{W}_{Xi}, \boldsymbol{W}_{Wi}, \boldsymbol{W}_{Yi}, \boldsymbol{W}_{Vi}] = [(\boldsymbol{\phi}_{Xi}, \boldsymbol{\rho}_{Xi}, \boldsymbol{b}_{Xi}), (\boldsymbol{\phi}_{Wi}, \boldsymbol{\rho}_{Wi}, \boldsymbol{b}_{Wi}), (\boldsymbol{\phi}_{Yi}, \boldsymbol{\rho}_{Yi}, \boldsymbol{b}_{Yi}), (\boldsymbol{\phi}_{Vi}, \boldsymbol{\rho}_{Vi}, \boldsymbol{b}_{Vi})]$
Output: The best GA values is represented as WBest-GA
Initialization
Form weight vector W, i.e., a real numbers to denote a chromosome as:
Initialize P,Set the declarations and generation
Evaluation of Fitness
To calculate the fitness E using Eq. (5)
Ranking
For smartness of the fitness values, rank each Win terms of P
Termination
Procedure terminates, when
Fitness= E= 10–20,TolCon = 10–18, Generations → 50, TolFun = 10–18
StallGenLimit → 100,PopulationSize → 300
Other values: default.
Go to [storage],
Ranking
Rank each W in population P for the quality of the fitness$E$
Reproduction
Selection=~selectionuniform.
Mutations= ~mutationadaptfeasible
Crossover=~crossoverheuristic.
Elitism= ~The best individuals ranked of "P"
Continue [fitnessevaluation]step
Storage
Save WBest-GA, the value of fitness E, time, function count and generation
GA Process End
Procedure of SQP Start
Inputs
Start point: WBest-GA
Output
The best GA-SQP values are shown as WGA-SQP
Initialize
Bounded restrictions; assignments; generations; and other announced values.
Terminate
Terminate when to get:
Fitness = 10–20, MaxFunEvals = 270000, Generations = 800,
TolCon = TolX = TolFun ≤ 10–22
While (termination)
Fitness evaluation
To evaluate the Fit values from the W
Adjustments
Invoke "fmincon" for the SQP. Adapt weight vector W for the E
generations of SQP. Compute fit
from the updated W
Store
Accumulate the weight vector WGA-SQP vector, E i.e., time of fitness,
counts of function and iterations for the current runs of SQP.
SQP Procedure End
Data Generations
Repeat 100 times this iterative process of GA-SQP to achieve a massive data-set of the optimization variables of ANNs for solving the nonlinear HIV model

Using the above network (4), an error functionEis given as:

$$E = E_1 + E_2 + E_3 + E_4 + E_5, \tag{5}$$

$$E_1 = \frac{1}{N}\sum_{m=1}^{N}\left(\widehat{X'}_m + \alpha\widehat{X}_m + d\widehat{X}_m - \mu\right)^2, \tag{6}$$

$$E_2 = \frac{1}{N}\sum_{m=1}^{N}\left(\widehat{W'}_m + (q-1)\alpha\widehat{X}_m\widehat{V}_m + e\widehat{W}_m + \lambda\widehat{W}_m\right)^2, \tag{7}$$

$$E_3 = \frac{1}{N}\sum_{m=1}^{N}\left(\widehat{Y'}_m - \lambda\widehat{W}_m + a\widehat{Y}_m - q\alpha\widehat{X}_m\widehat{V}_m\right)^2, \tag{8}$$

$$E_4 = \frac{1}{N}\sum_{m=1}^{N}\left(\widehat{V'}_m + \widehat{V}_m - k\widehat{Y}_m\right)^2, \tag{9}$$

$$E_5 = \frac{1}{4}\left(\left(\widehat{X}_0 - I_1\right)^2 + \left(\widehat{W}_0 - I_2\right)^2 + \left(\widehat{Y}_0 - I_3\right)^2 + \left(\widehat{V}_0 - I_4\right)^2\right), \tag{10}$$

where $Nh = 1$, $t_m = mh$, $\widehat{X}_m = \widehat{X}(t_m)$, $\widehat{W}_m = \widehat{W}(t_m)$, $\widehat{Y}_m = \widehat{Y}(t_m)$, $\widehat{V}_m = \widehat{V}(t_m)$The approximate results for susceptible X , infected W, recovered Y, and latently infected V classes are denoted as $\widehat{X}_m$, $\widehat{W}_m$, $\widehat{Y}_m$ and $\widehat{V}_m$, respectively. Accordingly, E_1, E_2, $E_3$and E_4show the error functions linked to differential forms of the HIV system (1), while, E_5 is the error function associated with the initial conditions. The approximate proposed results can be attained from the accessible best weights for which the error functions shown in Eq. (4) approaches to zero.

Optimization procedure: GA-SQP

The proficient weights based on ANNs by combining the integrated strength of meta-heuristic computing system for GA improved with SQP, i.e., 'GA-SQP'.

The competent global search scheme, i.e., GAs, presented by Holand at the last of the 19th century [37,38]. GA is applied for the weight vector $\boldsymbol{W}$ of ANN. The population formulation with candidate outcomes is attained using the real numbers. While, each distinct or candidate result is equal to unknown weights in ANN. GAs incorporated on the bases of its valuable components 'crossover', 'selection', 'mutation' and 'elitism'. Some well-known recent submissions of GA are cost optimized for a multi-energy source [39], development of emergency humanitarian logistics [40], glass transitions in boiling candies [41], applications of traveling salesman [42], building envelope project for populations [43], the optimal set of intersecting clusters [44], nanofluids models [45], execution in detection models [46], queen based models optimization [47], to optimize the heterogeneous bin packing [48] and to present the military surveillance design systems [49].

GA combined with the rapid local search scheme for rapid convergence by allocating the best GA values as a starting initial guess. Thus, effective local based scheme SQP is useful to fine-tune of the parameters. SQP has various applications, like as dynamic of bipedal walking robot [50],economic load dispatch problems [51], economic production of multiproduct [52], system of heating in quick thermal cycling blow mold [53], guide wire deformation analysis in the blood vessels [54], temporary hydrothermal coordination [55], recovery of flight vector for aircraft transport [56], LNG process [57], damage localization at wind turbine support structures [58], problems of optimal power flow [59] and the solution of convex quadratic bi-level programming models [60]. In this work, the hybridization of GA-SQP is used for the solution of the nonlinear HIV model. The detail pseudo code step of GA-SQP is given in Table 1.

Performance assessments

The performance gages for the HIV nonlinear model represented in Eq. 1based on Theil's inequality coefficient (TIC), root 'mean square error (RMSE)' and 'mean absolute error (MAE)'. The mathematical symbolizations of these operatives are represented as:

$$[\mathrm{TIC}_X, \mathrm{TIC}_W, \mathrm{TIC}_Y, \mathrm{TIC}_V] = \begin{pmatrix} \dfrac{\sqrt{\frac{1}{m}\sum_{i=1}^{m}\left(X_i-\widehat{X}_i\right)^2}}{\left(\sqrt{\frac{1}{m}\sum_{i=1}^{m}X_i^2}+\sqrt{\frac{1}{m}\sum_{i=1}^{m}\widehat{X}_i^2}\right)}, & \dfrac{\sqrt{\frac{1}{m}\sum_{i=1}^{m}\left(W_i-\widehat{W}_i\right)^2}}{\left(\sqrt{\frac{1}{m}\sum_{i=1}^{m}W_i^2}+\sqrt{\frac{1}{m}\sum_{i=1}^{m}\widehat{W}_i^2}\right)}, \\ \dfrac{\sqrt{\frac{1}{m}\sum_{i=1}^{m}\left(Y_i-\widehat{Y}_i\right)^2}}{\left(\sqrt{\frac{1}{m}\sum_{i=1}^{m}Y_i^2}+\sqrt{\frac{1}{m}\sum_{i=1}^{m}\widehat{Y}_i^2}\right)}, & \dfrac{\sqrt{\frac{1}{m}\sum_{i=1}^{m}\left(V_i-\widehat{V}_i\right)^2}}{\left(\sqrt{\frac{1}{m}\sum_{i=1}^{m}V_i^2}+\sqrt{\frac{1}{m}\sum_{i=1}^{m}\widehat{V}_i^2}\right)} \end{pmatrix}, \tag{11}$$

$$[\mathrm{RMSE}_X, \mathrm{RMSE}_W, \mathrm{RMSE}_Y, \mathrm{RMSE}_V] = \begin{bmatrix} \sqrt{\frac{1}{m}\sum_{i=1}^{m}\left(X_i-\widehat{X}_i\right)^2}, & \sqrt{\frac{1}{m}\sum_{i=1}^{m}\left(W_i-\widehat{W}_i\right)^2} \\ \sqrt{\frac{1}{m}\sum_{i=1}^{m}\left(Y_i-\widehat{Y}_i\right)^2}, & \sqrt{\frac{1}{m}\sum_{i=1}^{m}\left(V_i-\widehat{V}_i\right)^2} \end{bmatrix}, \tag{12}$$

$$[MAD_X, MAD_W, MAD_Y, MAD_V] = \begin{bmatrix} \frac{1}{m}\sum_{i=1}^{m}\left|X_i-\widehat{X}_i\right|, \frac{1}{m}\sum_{i=1}^{m}\left|W_i-\widehat{W}_i\right|, \\ \frac{1}{m}\sum_{i=1}^{m}\left|Y_i-\widehat{Y}_i\right|, \quad \frac{1}{m}\sum_{i=1}^{m}\left|V_i-\widehat{V}_i\right| \end{bmatrix} \tag{13}$$

The fitness function of the above HIV model (14) is shown as:

Optimization of the HIV model (1) is maintained by the hybrid of GA-SQP for hundred numbers of runs using 10 neurons to accomplish the system parameters. The set of best weights is provided to achieve the approximate values for the HIV model (1). The mathematical formulation of the approximate values becomes as:

$$E = \frac{1}{N}\sum_{m=1}^{N}\left(\begin{array}{c}\left[\widehat{X}'_m - 0.4 + 0.01{*}\widehat{X}_m + 0.04{*}\widehat{X}_m\widehat{V}_m\right]^2 + \left[\widehat{W}'_m - 0.008{*}\widehat{X}_m\widehat{V}_m + 0.4{*}\widehat{V}_m\right]^2 + \\ \left[\widehat{Y}'_m - 0.3{*}\widehat{W}_m + 0.2{*}\widehat{Y}_m - 0.032{*}\widehat{X}_m{*}\widehat{V}_m\right]^2 + \left[\widehat{V}'_m + 0.03\widehat{V}_m - 0.6{*}\widehat{Y}_m\right]^2\end{array}\right) + \frac{1}{4}\left(\left(\widehat{X}_0-7\right)^2 + \left(\widehat{W}_0-2\right)^2 + \left(\widehat{Y}_0-1\right)^2 + \left(\widehat{V}_0-4\right)^2\right), \tag{15}$$

Results and discussion

This section provides the detailed discussion for solving the HIV model given in Eq. (1) using 10 neurons. The relative study with Runge-Kutta results is provided to show the correctness and exactness of the proposed MW-ANN-GA-SQP. Moreover, statistical based results are accomplished to form the accuracy and precision.

Infection model based on HIV

The efficient form of the HIV model involving latently infected cells (IC) given in Eq. (1) by using different values provided in the literature based on the HIV infection model [10] as given in Table 2

The updated form of the model (1), using the above table values is given as:

$$\begin{cases} X'(t) = 0.4 - 0.01X - 0.04XV, & X(0) = 7 \\ W'(t) = 0.008XV - 0.4W, & W(0) = 2 \\ Y'(t) = 0.3W - 0.2Y + 0.032XV, & Y(0) = 1 \\ V'(t) = -0.03V + 0.6Y, & V(0) = 4 \end{cases} \tag{14}$$

$$\begin{aligned}\widehat{X}(t) = {} & 0.0277cos(1.75(1.2541t + 0.5959))e^{-0.5(1.2541t+0.5959)^2} \\ & -0.3640cos(1.75(1.0005t + 2.3692))e^{-0.5(1.0005t+2.3692)^2} \\ & +0.3479cos(1.75(-0.957t - 1.6996))e^{-0.5(-0.957t-1.6996)^2} \\ & +.... + 0.2947cos(1.75(0.6385t + 0.4466))e^{-0.5(0.6385x+0.4466)^2}\end{aligned} \tag{16}$$

$$\begin{aligned}\widehat{W}(t) = {} & 0.3430cos(1.75(0.1120t - 0.3491))e^{-0.5(0.1120t-0.3491)^2} \\ & -0.1062cos(1.75(1.7497t + 1.1354))e^{-0.5(1.7497t+1.1354)^2} \\ & -0.0105cos(1.75(3.0663t + 3.4108))e^{-0.5(3.0663t+3.4108)^2} \\ & +.... + 1.0215cos(1.75(-0.238t - 0.0919))e^{-0.5(-0.238t-0.0919)^2}\end{aligned} \tag{17}$$

$$\begin{aligned}\widehat{Y}(t) = {} & -0.0103cos(1.75(2.1909t + 1.0006))e^{-0.5(2.1909t+1.0006)^2} \\ & -1.2340cos(1.75(0.6904t + 1.1908))e^{-0.5(0.6904t+1.1908)^2} \\ & +0.3644cos(1.75(2.1849t + 2.7584))e^{-0.5(2.1849t+2.7584)^2} \\ & +.... + 1.0215cos(1.75(-0.238t - 0.0919))e^{-0.5(-0.238t-0.0919)^2}\end{aligned} \tag{18}$$

Table 2
List of parameters used to study the HIV based infection model.

Parameter	Description	Values [10]
μ	UR of CD4$^+$T cells	0.4
λ	Rate of recovery of IC	0.3
d	Death UR of CD4$^+$T cells	0.01
q	Removal rate of recombinants	0.8
S_1	IVs of UR of CD4$^+$T cells	7
S_2	IVs of infected CD4$^+$T cells	2
S_3	IVs of Virus free cells	1
S_4	IVs of latently IC	4
α	Increased infection rate	0.04
e	Rate of infection of recombinants	0.1
a	Death rate values of virus free cells	0.2
u	Death rate values of latently IC	0.03

$$\begin{aligned}\widehat{V}(t) &= 4.1003cos(1.75(0.1473t-0.6740))e^{-0.5(0.1473t-0.6740)^2}\\ &-0.7278cos(1.75(0.5874t+0.1598))e^{-0.5(0.5874t+0.1598)^2}\\ &+0.4354cos(1.75(0.1541t-0.5522))e^{-0.5(0.1541t-0.5522)^2}\\ &+.... -0.8573cos(1.75(0.5221t-0.7810))e^{-0.5(0.5221t-0.7810)^2}\end{aligned} \tag{19}$$

The graphic designs using GA-SQP using the parameters of the model (14) are plotted through Figs. 2–7 using 10 neurons based on the mathematical modelling of ANN. The set of trained weights for $X(t)$;$W(t)$; $Y(t)$ and $V(t)$ denoting the best values of the fitness for 10 neurons are expressed in Fig. 2. The result plots of the proposed method MW-ANN-GA-SQP and Runge-Kutta scheme are provided in Fig. 3.The results obtained by the stochastic and traditional methodologies are overlapped, which indicate the validity and correctness of the designed MW-ANN-GA-SQP. The values of the absolute error (AE) are calculated for $X(t)$ and $W(t)$ in the first portion of the Fig. 4, whereas in the second half of Fig. 4, the AE values for $Y(t)$ and $V(t)$ are calculated. The existing outcomes are compared with the Runge-Kutta results. In Fig. 4, the comparison of the obtained results with the standard Runge-Kutta values using 10 numbers of neurons in ANN models are given. It is depicted in Fig. 4(a), that the AE values for $X(t)$ and $W(t)$ lie around 10^{-06} to 10^{-08} and 10^{-07} to 10^{-08}, respectively. Although the values of AE for $Y(t)$ and $V(t)$ lie in the ranges of 10^{-07} to 10^{-08} and 10^{-05} to 10^{-07}, respectively. The first portion of the Fig. 4 shows the comparison for $X(t)$ and $W(t)$, while the second portion is related to the values of $Y(t)$ and $V(t)$. The matching results of the current solutions with the Runge-Kutta numerical values show the precision and accuracy of the MW-ANN-GA-SQP.

The performance values of the statistical gages TIC, RMSE and MAD along with the box plots and histogram are narrated in Figs. 5–7. It is observed on the behalf of the statistical results that most of the values of TIC lie between 10^{-09} to 10^{-10}, while most of the values of RMSE and MAD lie around 10^{-05} to 10^{-07}. One may conclude from these outcomes that 90% or more of independent trials attained the reasonable and

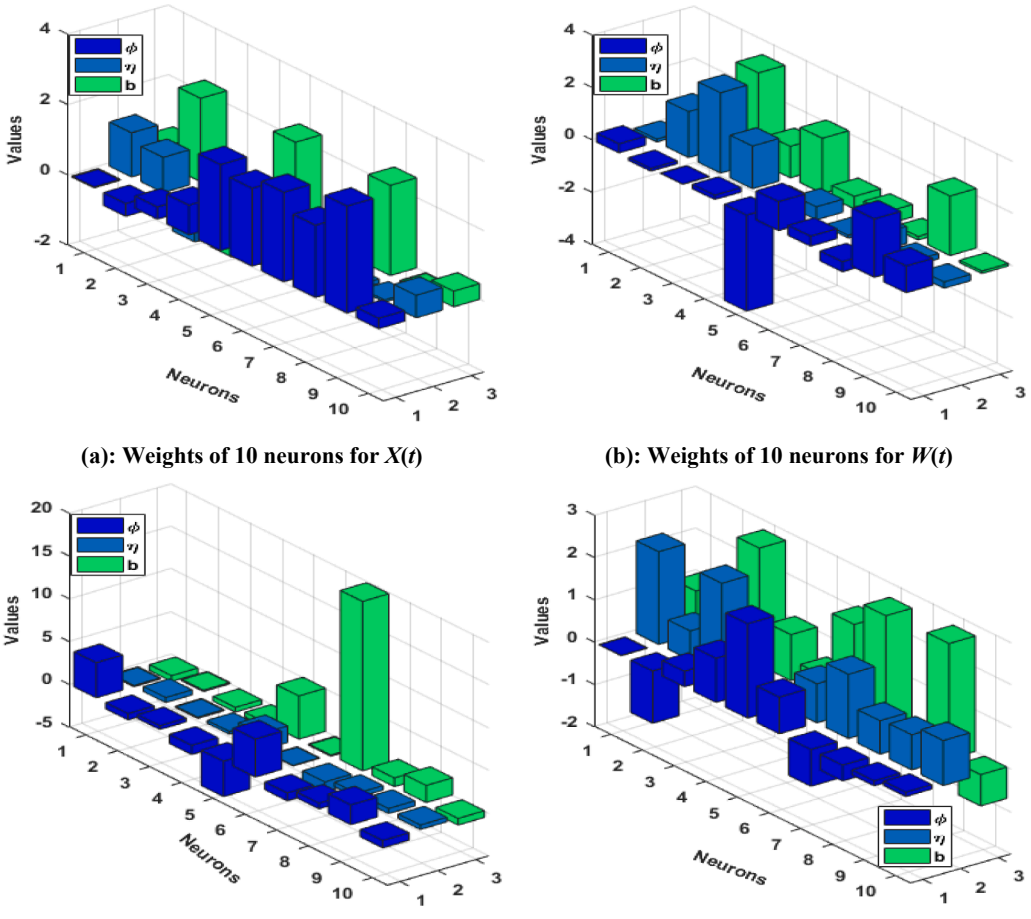

(a): Weights of 10 neurons for $X(t)$ **(b): Weights of 10 neurons for $W(t)$**

(c): Weights of 10 neurons for $Y(t)$ **(d): Weights of 10 neurons for $V(t)$**

Fig. 2. Trained weights of MW-ANN for the best merit achieved.

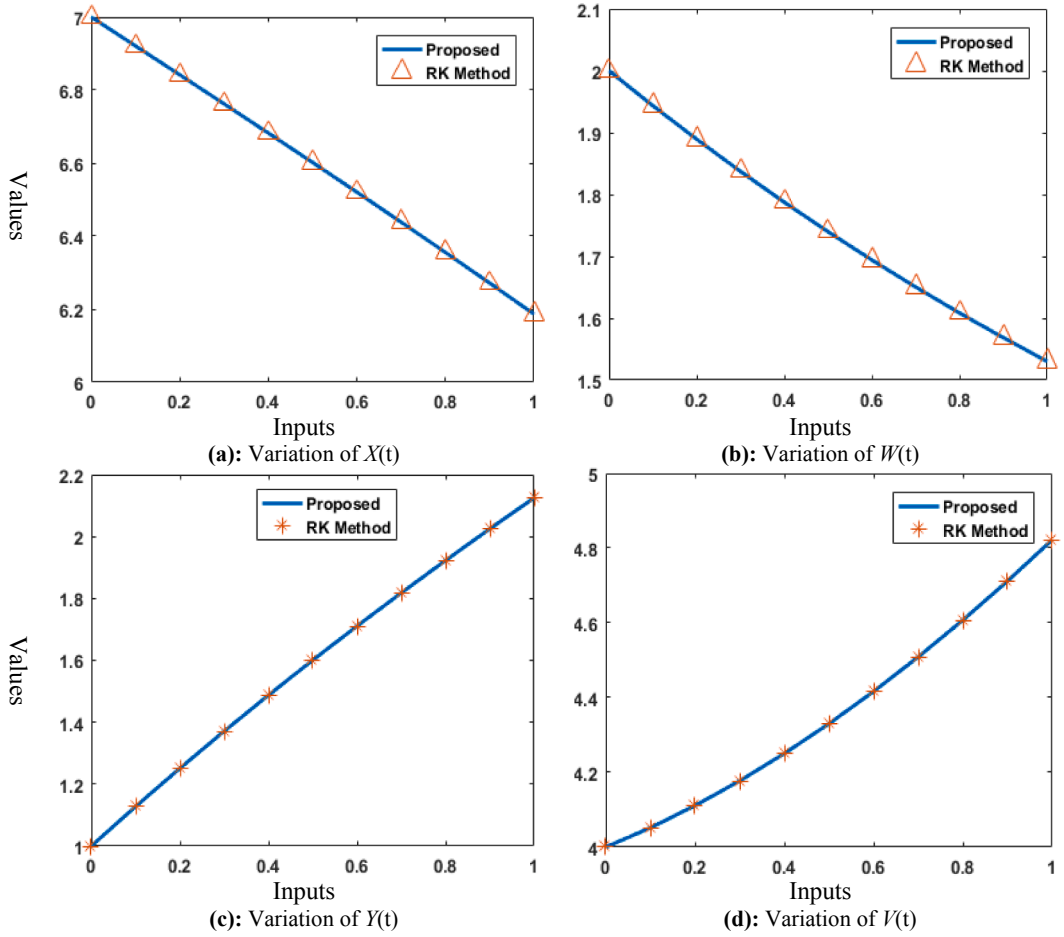

Fig. 3. Results of biological HIV virus infection model.

precise level of the statistical TIC measures. However, the level is about80% in case of MAD and RMSE metrics.

For strengthening the accuracy as well as convergence of the MW-ANN-GA-SQP, the precision analysis is observed based on the minimum (Min), 'semi interquartile range (SIR)' and median (Med). The statistical results in Min, SIR and Med for $X(t)$ and $W(t)$ are tabulated in Table 3, while the results for $Y(t)$ and $V(t)$ is drawn in Table 4. The scale of Min, Med and SIR values for all indexes lies around 10^{-08} to 10^{-11}, 10^{-06} to 10^{-08} and 10^{-06} to 10^{-07}, respectively.

Conclusions

In this study, the Morlet wavelet artificial neural network is designed to solve the biological HIV infection system of latently infected cells. An error-based fitness function design by using the capability of differential system and boundary conditions. The optimization of this designed error-based function is performed by using the heuristic capability of genetic algorithm and fast local search sequential quadratic algorithm. The designed computing solver MW-ANN-GA-SQP is efficiently implemented to solve the biological HIV infection spread model. The accurate performance of the MW-ANN-GA-SQP is observed by comparing the obtained results and the reference solutions. The plots of the solution, AE along with statistical illustrations of the TIC, RMSE and MAD are drawn in satisfactory measures. The statistical performances based on 100 executions indicate the reliability of the MW-ANN-GA-SQP to solve the HIV infection model. Moreover, the magnitudes of mean, median, semi-interquartile ranges authenticate the precision, trustworthiness and robustness of the MW-ANN-GA-SQP. In the future, the proposed MW-ANN-GA-SQP looks capable to solve the biological nonlinear systems [61–63] and nonlinear fluid dynamic systems [64–68] and also some others [69–87].

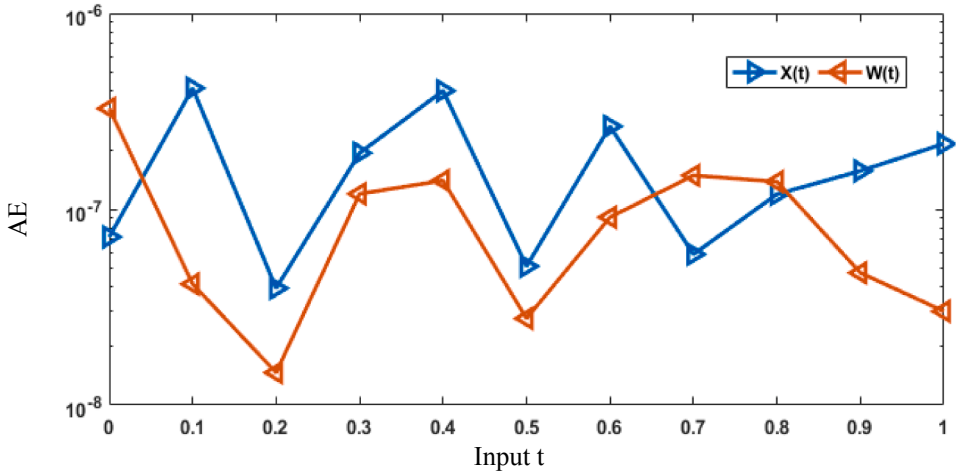

(a): AE valuesfor 10 neurons for $X(t)$ and $W(t)$

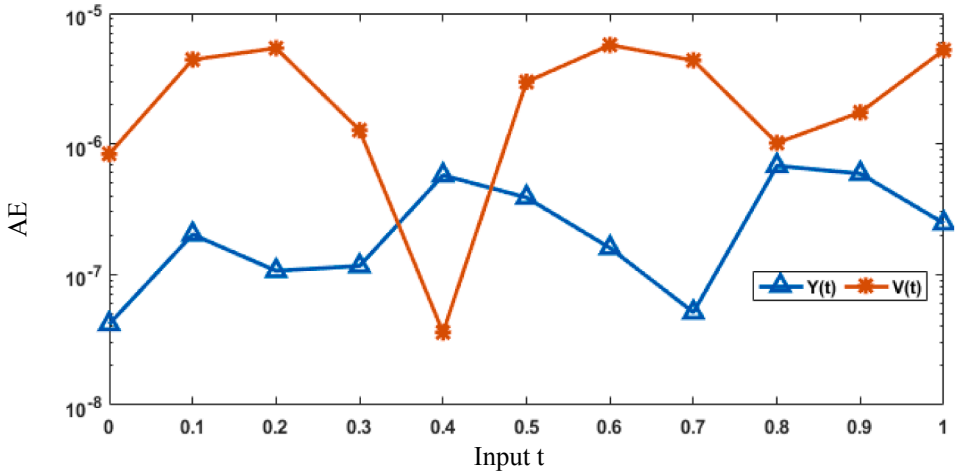

(b):AE values for 10 neurons for $Y(t)$ and $V(t)$

Fig. 4. Comparative study of AE values for 10 neurons.

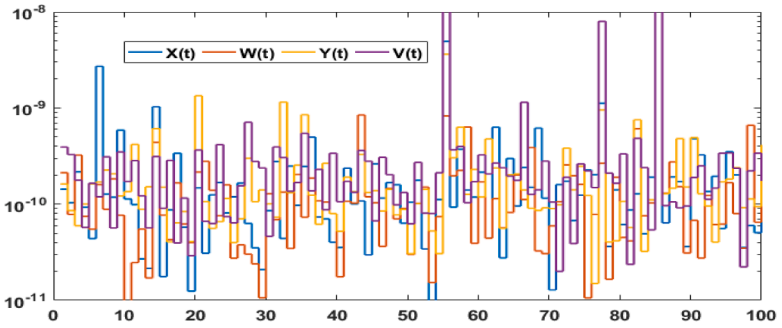

Convergence measures on TIC for $X(t)$,$W(t)$, $Y(t)$ and $V(t)$

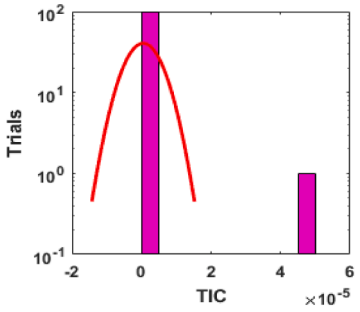

(a): Histogramsof $X(t)$

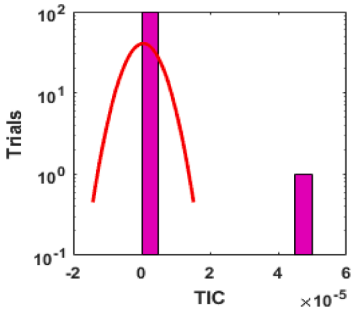

(b): Histograms of $W(t)$

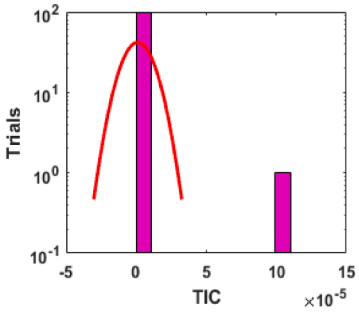

(c): Histograms of$Y(t)$

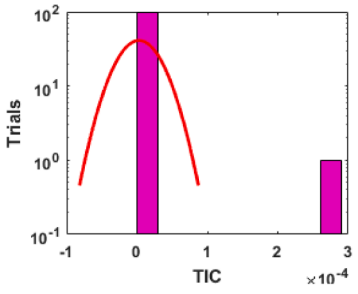

(d): Histogram for $V(t)$

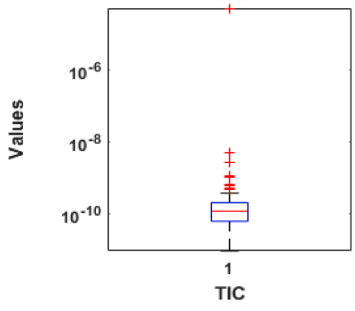

(e): Box plot for $X(t)$

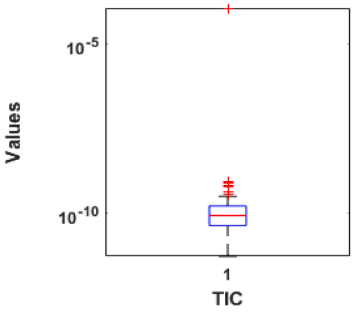

(f): Box plot for $W(t)$

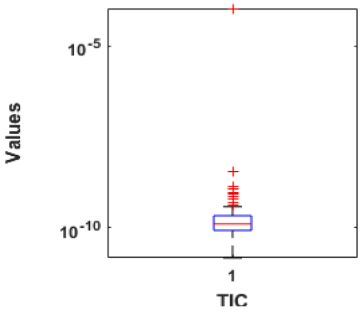

(g): Box plots of $Y(t)$

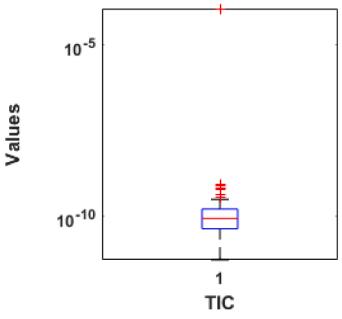

(h): Box plot of $V(t)$

Fig. 5. Statistics procedures for TIC using the histograms/box plots.

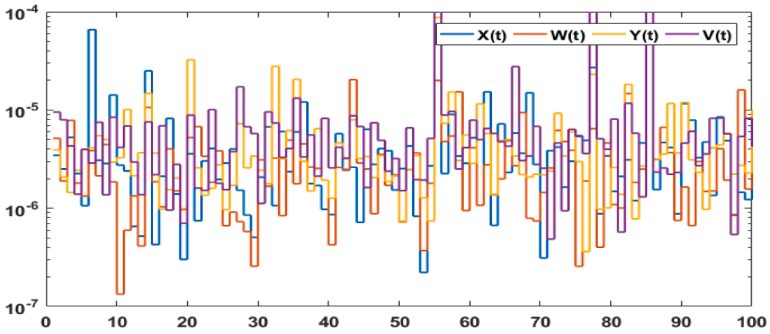

Convergence measures on RMSE for $X(t)$,$W(t)$, $Y(t)$ and $V(t)$

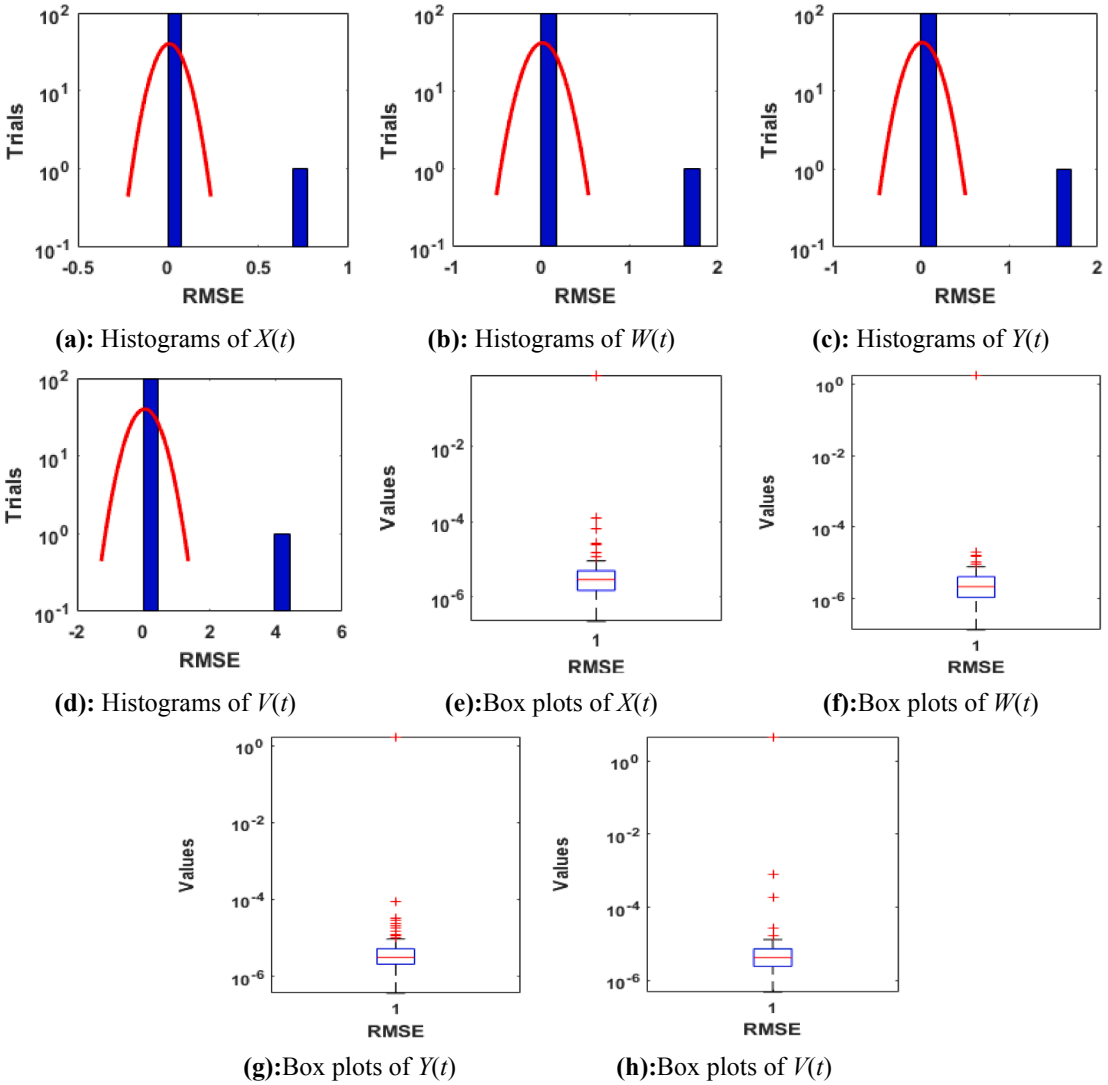

(a): Histograms of $X(t)$ **(b):** Histograms of $W(t)$ **(c):** Histograms of $Y(t)$

(d): Histograms of $V(t)$ **(e):**Box plots of $X(t)$ **(f):**Box plots of $W(t)$

(g): Box plots of $Y(t)$ **(h):**Box plots of $V(t)$

Fig. 6. Statistics procedures for RMSE with the histogram and box plots for 10 neurons.

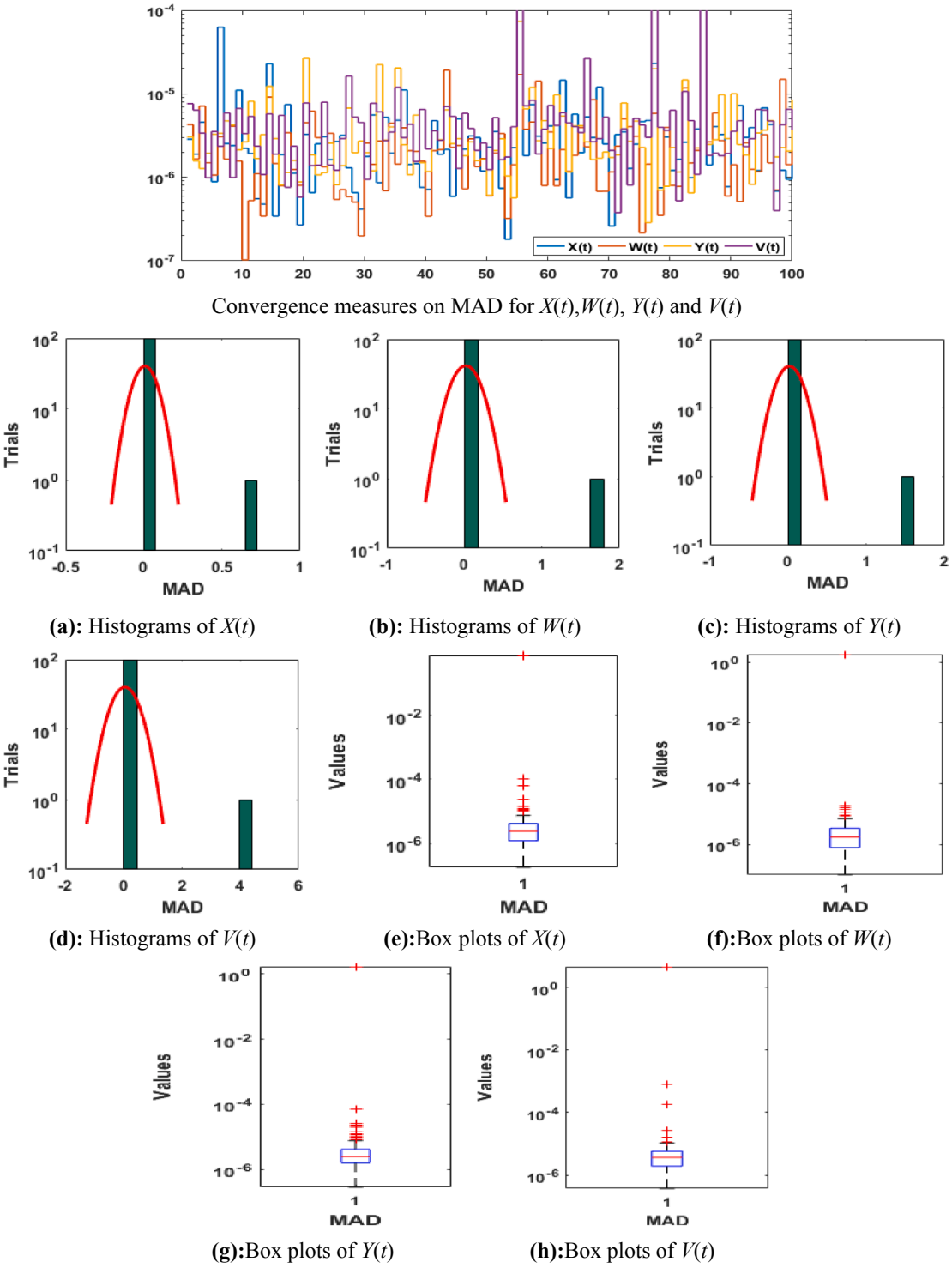

Convergence measures on MAD for $X(t)$,$W(t)$, $Y(t)$ and $V(t)$

(a): Histograms of $X(t)$ **(b):** Histograms of $W(t)$ **(c):** Histograms of $Y(t)$

(d): Histograms of $V(t)$ **(e):**Box plots of $X(t)$ **(f):**Box plots of $W(t)$

(g): Box plots of $Y(t)$ **(h):**Box plots of $V(t)$

Fig. 7. Statistics procedures for MAD with the histogram and box plots for 10 neurons.

Table 3
Statistics results for $X(t)$ and $W(t)$.

t	$X(t)$			$W(t)$		
	Min	Median	SIR	Min	Median	SIR
0	7.421E-10	1.510E-07	3.221E-07	9.927E-11	9.566E-08	1.858E-07
0.1	7.602E-08	2.937E-06	2.144E-06	2.567E-08	2.043E-06	2.244E-06
0.2	3.951E-08	3.665E-06	2.761E-06	1.465E-08	2.728E-06	2.334E-06
0.3	2.651E-08	1.870E-06	2.070E-06	1.426E-08	1.303E-06	1.506E-06
0.4	6.387E-09	1.487E-06	1.439E-06	2.013E-09	1.128E-06	1.143E-06
0.5	1.971E-08	1.714E-06	1.939E-06	1.281E-08	1.569E-06	1.600E-06
0.6	3.299E-09	1.874E-06	1.614E-06	9.106E-08	2.172E-06	1.695E-06
0.7	3.746E-09	2.531E-06	1.547E-06	4.991E-08	1.823E-06	1.816E-06
0.8	5.097E-09	2.440E-06	2.184E-06	2.011E-08	2.089E-06	1.817E-06
0.9	1.472E-08	1.803E-06	1.503E-06	1.369E-08	1.285E-06	1.287E-06
1	7.150E-08	2.224E-06	1.801E-06	1.548E-09	1.885E-06	1.576E-06

Table 4
Statistics based outcomes for $Y(t)$ and $V(t)$.

t	$X(t)$			$W(t)$		
	Min	Median	SIR	Min	Median	SIR
0	1.020E-09	1.503E-07	2.513E-07	4.277E-10	1.525E-07	2.813E-07
0.1	2.621E-08	3.599E-06	1.827E-06	2.041E-08	4.338E-06	2.164E-06
0.2	4.770E-08	4.207E-06	3.017E-06	3.278E-08	5.770E-06	5.121E-06
0.3	7.338E-08	1.886E-06	1.386E-06	1.727E-08	3.091E-06	4.136E-06
0.4	2.688E-08	8.841E-07	8.204E-07	2.317E-08	1.635E-06	1.321E-06
0.5	2.640E-09	2.220E-06	1.333E-06	2.221E-08	2.144E-06	1.400E-06
0.6	1.414E-08	3.283E-06	2.277E-06	3.994E-08	2.191E-06	1.396E-06
0.7	1.177E-08	2.949E-06	1.901E-06	1.201E-07	4.870E-06	3.358E-06
0.8	1.483E-08	2.304E-06	1.831E-06	1.178E-07	5.716E-06	4.977E-06
0.9	1.145E-08	1.633E-06	1.488E-06	1.321E-07	3.166E-06	1.838E-06
1	1.919E-08	3.315E-06	2.440E-06	1.059E-09	2.723E-06	2.181E-06

Funding

National Natural Science Foundation of China (No. 71601072), Key Scientific Research Project of Higher Education Institutions in Henan Province of China (No. 20B110006) and the Fundamental Research Funds for the Universities of Henan Province (No. NSFRF210314).

Declaration of Competing Interest

The authors declare that they have no known competing financial interests or personal relationships that could have appeared to influence the work reported in this paper.

References

[1] Rosenberg ES, Altfeld M, Poon SH, Phillips MN, Wilkes BM, Eldridge RL, et al. Immune control of HIV-1 after early treatment of acute infection. Nature 2000;407(6803):523.
[2] Perelson AS, Kirschner DE, De Boer R. Dynamics of HIV infection of CD4+ T cells. Math Biosci 1993;114(1):81–125.
[3] Perelson AS. Modeling the interaction of the immune system with HIV. In: Mathematical and statistical approaches to AIDS epidemiology. Berlin, Heidelberg: Springer; 1989. p. 350–70.
[4] Ali N, Zaman G. Asymptotic behavior of HIV-1 epidemic model with infinite distributed intracellular delays. SpringerPlus 2016;5(1):324.
[5] Hattaf K. Spatiotemporal dynamics of a generalized viral infection model with distributed delays and CTL immune response. Computation 2019;7(2):21.
[6] Hattaf K, Yousfi N. Modeling the adaptive immunity and both modes of tr ANN mission in HIV infection. Computation 2018;6(2):37.
[7] Wang L, Li MY. Mathematical analysis of the global dynamics of a model for HIV infection of CD4+ T cells. Math Biosci 2006;200(1):44–57.
[8] Ali N, Zaman G, Algahtani O. Stability analysis of HIV-1 model with multiple delays. Adv Difference Eq 2016;2016(1):88.
[9] Guerrero-Sánchez Y, Umar M, Sabir Z, Guirao JL, Raja MAZ. Solving a class of biological HIV infection model of latently infected cells using heuristic approach. Discr Cont Dyn Syst-S 2020.
[10] Umar M, Sabir Z, Amin F, Guirao JL, Raja MAZ. Stochastic numerical technique for solving HIV infection model of CD4+ T cells. Eur Phys J Plus 2020;135(6):403.
[11] Zibaei S, Namjoo M. A nonstandard finite difference scheme for solving fractional-order model of HIV-1 infection of CD4$^+$ t-cells. Iranian J Mathem Chem 2015;6(2):169–84.
[12] Prague M. Use of dynamical models for treatment optimization in HIV infected patients: a sequential Bayesian analysis approach; 2016.
[13] Venkatesh SG, Balachandar SR, Ayyaswamy SK, Balasubramanian K. A new approach for solving a model for HIV infection of CD4$^+$ t-cells arising in mathematical chemistry using wavelets. J Math Chem 2016;54(5):1072–82.
[14] Ghoreishi M, Ismail AM, Alomari AK. Application of the homotopy analysis method for solving a model for HIV infection of CD4+ T-cells. Math Comput Modell 2011;54(11–12):3007–15.
[15] Yüzbaşı Ş. A numerical approach to solve the model for HIV infection of CD4+ T cells. Appl Math Model 2012;36(12):5876–90.
[16] Srivastava VK, Awasthi MK, Kumar S. Numerical approximation for HIV infection of CD4+ T cells mathematical model. Ain Shams Eng J 2014;5(2):625–9.
[17] Sabir Z, Baleanu D, Shoaib M, Raja MAZ. Design of stochastic numerical solver for the solution of singular three-point second-order boundary value problems. Neural Comput Appl 2020:1–17.
[18] Sabir Z, Raja MAZ, Khalique CM, Unlu C. Neuro-evolution computing for nonlinear multi-singular system of third order Emden-Fowler equation. Math Comput Simul 2021;185:799–812.
[19] Fateh MF, et al. Differential evolution based computation intelligence solver for elliptic partial differential equations. Front Inf Technol Electr Eng 2019;20(10):1445–56.
[20] Sabir Z, Raja MAZ, Guirao JL, Shoaib M. A neuro-swarming intelligence based computing for second order singular periodic nonlinear boundary value problems.
[21] Umar M, Sabir Z, Raja MAZ, Amin F, Saeed T, Guerrero-Sanchez Y. Integrated neuro-swarm heuristic with interior-point for nonlinear SITR model for dynamics of novel COVID-19. Alexandria Eng J 2021;60(3):2811–24.
[22] Umar M, et al. Intelligent computing for numerical treatment of nonlinear prey–predator models. Appl Soft Comput 2019;80:506–24.
[23] Umar M, Sabir Z, Zahoor Raja MA, Gupta M, Le DN, Aly AA, et al. Computational intelligent paradigms to solve the nonlinear SIR system for spreading infection and treatment using Levenberg–Marquardt Backpropagation. Symmetry 2021;13(4):618.
[24] Sabir Z, Guirao JL, Saeed T. Solving a novel designed second order nonlinear Lane-Emden delay differential model using the heuristic techniques. Appl Soft Comput 2021;102:107105.
[25] Sabir Z, Amin F, Pohl D, Guirao JL. Intelligence computing approach for solving second order system of the Emden-Fowler model. J Intell Fuzzy Syst 2020:1–16.
[26] Sabir Z, Raja MAZ, Guirao JL, Shoaib M. A novel design of fractional Meyer wavelet neural networks with application to the nonlinear singular fractional Lane-Emden systems. Alexandria Eng J 2021;60(2):2641–59.
[27] Raja MAZ, Shah FH, Khan AA, Khan NA. Design of bio-inspired computational intelligence technique for solving steady thin film flow of Johnson-Segalman fluid on vertical cylinder for drainage problems. J Taiwan Inst Chem Eng 2016;60:59–75.
[28] Sabir Z, Zahoor Raja MA, Baleanu D. Fractional Mayer Neuro-swarm heuristic solver for multi-fractional Order doubly singular model based on Lane-Emden equation. Fractals 2021.

[29] Sabir Z, Raja MAZ, Umar M, Shoaib M. Neuro-swarm intelligent computing to solve the second-order singular functional differential model. Eur Phys J Plus 2020;135(6):474.
[30] Sabir Z, Wahab HA, Umar M, Erdoğan F. Stochastic numerical approach for solving second order nonlinear singular functional differential equation. Appl Math Comput 2019;363:124605.
[31] Raja MAZ, Farooq U, Chaudhary NI, Wazwaz AM. Stochastic numerical solver for nanofluidic problems containing multi-walled carbon nanotubes. Appl Soft Comput 2016;38:561–86.
[32] Sabir Z, et al. Neuro-heuristics for nonlinear singular Thomas-Fermi systems. Appl Soft Comput 2018;65:152–69.
[33] Raja MAZ, Mehmood J, Sabir Z, Nasab AK, Manzar MA. Numerical solution of doubly singular nonlinear systems using neural networks-based integrated intelligent computing. Neural Comput Appl 2019;31(3):793–812.
[34] Raja MAZ, Umar M, Sabir Z, Khan JA, Baleanu D. A new stochastic computing paradigm for the dynamics of nonlinear singular heat conduction model of the human head. Eur Phys J Plus 2018;133(9):364.
[35] Sabir Z, Raja MAZ, Umar M, Shoaib M. Design of neuro-swarming-based heuristics to solve the third-order nonlinear multi-singular Emden-Fowler equation. Eur Phys J Plus 2020;135(6):1–17.
[36] Sabir Z, Wahab HA, Umar M, Sakar MG, Raja MAZ. Novel design of Morlet wavelet neural network for solving second order Lane-Emden equation. Math Comput Simul 2020.
[37] Srinivas N, Deb K. Muilti-objective optimization using no dominated sorting in genetic algorithms. Evol Comput 1994;2(3):221–48.
[38] Zalzala AM. Genetic algorithms in engineering systems (Vol. 55). Iet; 1997.
[39] An PQ, Murphy MD, Breen MC, Scully T. One-day-ahead cost optimisation for a multi-energy source building using a genetic algorithm. In: 2016 UKACC 11th International Conference on Control (CONTROL). IEEE; 2016. p. 1–6.
[40] Chang FS. Greedy-Search-based Multi-Objective Genetic Algorithm for Emergency Humanitarian Logistics Scheduling; 2016.
[41] Tan J, Kerr WL. Determination of glass trANNitions in boiled candies by capacitance based thermal analysis (CTA) and genetic algorithm (GA). J Food Eng 2017;193:68–75.
[42] Vaishnav P, Choudhary N, Jain K. Traveling Salesman Problem Using Genetic Algorithm: A Survey; 2017.
[43] Lim YW, Majid HA, Samah AA, Ahmad MH, Ossen DR. BIM and Genetic Algorithm optimisation for sustainable building envelope design. In: Building information systems in the construction industry; 2018. p. 159.
[44] Das S, Chaudhuri S, Das AK. Optimal Set of Overlapping Clusters Using Multi-objective Genetic Algorithm. In Proceedings of the 9th International Conference on Machine Learning and Computing; 2017 (pp. 232–237). ACM.
[45] Azad AV, Azad NV. Application of nanofluids for the optimal design of shell and tube heat exchangers using genetic algorithm. Case Stud Therm Eng 2016;8:198–206.
[46] Resende PAA, Drummond AC. Adaptive anomaly-based intrusion detection system using genetic algorithm and profiling. Sec Privacy 2018;1(4):e36.
[47] Alharbi S, Venkat I. A genetic algorithm-based approach for solving the minimum dominating set of queens problem. J Optimiz; 2017.
[48] Sridhar R, Chandrasekaran M, Sriramya C, Tom Page. Optimization of heterogeneous Bin packing using adaptive genetic algorithm. In IOP Conference Series: Materials Science and Engineering, vol. 183, no. 1, p. 012026. IOP Publishing; 2017.
[49] Ball MG, Qela B, Wesolkowski S. A review of the use of computational intelligence in the design of military surveillance networks. In Recent Advances in Computational Intelligence in Defense and Security (pp. 663–693); 2016. Springer International Publishing.
[50] Sun Z, Tian Y, Li H, Wang J. A superlinear convergence feasible sequential quadratic programming algorithm for bipedal dynamic walking robot via discrete mechanics and optimal control. Optimal Control Appl Methods 2016;37(6):1139–61.
[51] Gul RN, Ahmad A, Fayyaz S, Sattar MK, Ul Haq SS. A hybrid flower pollination algorithm with sequential quadratic programming technique for solving dynamic combined economic emission dispatch problem. Mehran Univ Res J Eng Technol 2021;40(2):371–82.
[52] Pasandideh SHR, Niaki STA, Gharaei A. Optimization of a multiproduct economic production quantity problem with stochastic constraints using sequential quadratic programming. Knowl-Based Syst 2015;84:98–107.
[53] Xiao CL, Huang HX. Optimal design of heating system in rapid thermal cycling blow mold by a two-step method based on sequential quadratic programming. Int Commun Heat Mass Trans 2018;96:114–21.
[54] Li L, Tang Q, Tian Y, Wang W, Chen W, Xi F. Investigation of guidewire deformation in blood vessels based on an SQP algorithm. Appl Sci 2019;9(2):280.
[55] Chaudhry FA, Amin M, Iqbal M, Khan RD, Khan JA. A novel chaotic differential evolution hybridized with quadratic programming for short-term hydrothermal coordination. Neural Comput Appl 2018;30(11):3533–44.
[56] Engelbrecht JJ, Engelbrecht JA. Optimal attitude and flight vector recovery for large trANNport aircraft using sequential quadratic programming. In: Pattern Recognition Association of South Africa and Robotics and Mechatronics International Conference (PRASA-RobMech). IEEE; 2016. p. 1–7.
[57] Rehman A, Qyyum MA, Qadeer K, Zakir F, He X, Nawaz A, et al. Single mixed refrigerant LNG process: investigation of improvement potential, operational optimization, and real potential for further improvements. J Cleaner Prod 2021;284:125379.
[58] Schröder K, Gebhardt C, Rolfes R. Damage Localization at Wind Turbine Support Structures Using Sequential Quadratic Programming for Model Updating. In de 8th European Workshop On Structural Health Monitoring, Bilbao; 2016.
[59] Sivasubramani S, Swarup KS. Sequential quadratic programming based differential evolution algorithm for optimal power flow problem. IET Generat, Trannmis Distrib 2011;5(11):1149–54.
[60] Etoa JBE. Solving convex quadratic bilevel programming problems using an enumeration sequential quadratic programming algorithm. J Global Optim 2010;47(4):615–37.
[61] Guerrero Sánchez Y, Sabir Z, Günerhan H, Baskonus HM. Analytical and Approximate Solutions of a Novel Nervous Stomach Mathematical Model. Discrete Dynamics in Nature and Society; 2020.
[62] Umar M, Sabir Z, Raja MAZ, Shoaib M, Gupta M, Sánchez YG. A stochastic intelligent computing with neuro-evolution heuristics for nonlinear SITR system of novel COVID-19 dynamics. Symmetry 2020;12(10):1628.
[63] Sanchez YG, Sabir Z, Guirao JL. Design of a nonlinear SITR fractal model based on the dynamics of a novel coronavirus (COVID); 2020.
[64] Sajid T, Tanveer S, Munsab M, Sabir Z. Impact of oxytactic microorganisms and variable species diffusivity on blood-gold Reiner-Philippoff nanofluid. Appl Nanosci 2021;11(1):321–33.
[65] Ayub A, Wahab HA, Sabir Z, Arbi A. A note on heat transport with aspect of magnetic dipole and higher order chemical process for steady micropolar fluid. Fluid-Structure Interaction. IntechOpen; 2020.
[66] Sajid T, Sabir Z, Tanveer S, Arbi A, Altamirano GC. Upshot of radiative rotating Prandtl fluid flow over a slippery surface embedded with variable species diffusivity and multiple convective boundary conditions. Heat Transfer 2020.
[67] Sajid T, Tanveer S, Sabir Z, Guirao JLG. Impact of activation energy and temperature-dependent heat source/sink on maxwell–sutterby fluid. Mathematical Problems in Engineering; 2020.
[68] Sabir Z, Ayub A, Guirao JL, Bhatti S, Shah SZH. The effects of activation energy and thermophoretic diffusion of nanoparticles on steady micropolar fluid along with Brownian motion. Advances in Materials Science and Engineering; 2020.
[69] Cordero A, Jaiswal JP, Torregrosa JR. Stability analysis of fourth-order iterative method for finding multiple roots of non-linear equations. Appl Mathem Nonlinear Sci 2019;4(1):43–56.
[70] Yel G, Cattani C, Baskonus HM, Gao W. On the complex simulations with dark-bright to the Hirota-Maccari system. J Comput Nonlinear Dyn 2021. https://doi.org/10.1115/1.4050677.
[71] Eskitascioglu EI, Aktas MB, Baskonus HM. New complex and hyperbolic forms for Ablowitz-Kaup-Newell-Segur wave equation with fourth order. Appl Mathem Nonlinear Sci 2019;4(1):105–12.
[72] Li YM, Baskonus HM, Khudhur AM. Investigations of the complex wave patterns to the generalized Calogero-Bogoyavlenskii-Schiff equation. Soft Comput 2021. https://doi.org/10.1007/s00500-021-05627-2.
[73] Durur H, Yokus A. Exact solutions of (2+1)-Ablowitz-Kaup-Newell-Segur equation. Appl Mathem Nonlin Sci 2020. https://doi.org/10.2478/amns.2020.2.00074.
[74] Kumar A, Ilhan E, Ciancio A, Yel G, Baskonus HM. Extractions of some new travelling wave solutions to the conformable Date-Jimbo-Kashiwara-Miwa Equation. Aims Mathem 2021;6(5):4238–64.
[75] Ziane D, Cherif MH, Cattani C, Belghaba K. Yang-Laplace decomposition method for nonlinear system of local fractional partial differential equations. Appl Mathem Nonl Sci 2019;4(2):489–502.
[76] Arslan D. The comparison study of hybrid method with RDTM for solving Rosenau-Hyman equation. Appl Mathem Nonlin Sci 2020;5(1):267–74.
[77] Jhangeer A, Baskonus HM, Yel G, Gao W. New exact solitary wave solutions, bifurcation analysis and first order conserved quantities of resonance nonlinear Shrödinger's equation with Kerr law nonlinearity. J King Saud Univ – Sci 2021;33(1):101180.
[78] Arslan D. The numerical study of a hybrid method for solving telegraph equation. Appl Mathem Nonlinear Sci 2020;5(1):293–302.
[79] Çetinkaya A, Kiymaz O. The solution of the time-fractional diffusion equation by the generalized differential transform method. Math Comput Modell 2013;57(9–10):2349–54.
[80] Gao W, Veeresha P, Prakasha DG, Baskonus HM. New numerical simulation for fractional Benney-Lin equation arising in falling film problems using two novel techniques. Num Methods Partial Diff Eq 2021;37(1):210–43.
[81] Akganduller O, Atmaca SP. Discrete normal vector field approximation via time scale calculus. Appl Mathem Nonl Sci 2020;5(1):349–60.
[82] Gao W, Gunerhan H, Baskonus HM. Analytical and approximate solutions of an epidemic system of HIV/AIDS transmission. Alexandria Eng J 2020;59(5):3197–211.
[83] Dusunceli F. New exact solutions for generalized (3+1) shallow water-like (SWL) equation. Appl Mathem Nonlinear Sci 2019;4(2):365–70.
[84] Çetinkaya A, Kiymaz O, Agarwal P, Agarwal R. A comparative study on generating function relations for generalized hypergeometric functions via generalized fractional operators. Adv Diff Eq 2018;2018(1):1–11.
[85] Gao W, Ismael HF, Husien AM, Bulut H, Baskonus HM, Optical Soliton solutions of the Nonlinear Schrödinger and resonant nonlinear schrödinger equation with parabolic law, Appl Sci, 10(1), 219, 1–20, 2020.
[86] Yel G, Akturk T. A new approach to (3+1) dimensional Boiti–Leon–Manna–Pempinelli equation. Appl Mathem Nonlinear Sci 2020;5(1):309–16.
[87] Ali KK, Yilmazer R, Baskonus HM, Bulut H. Modulation instability analysis and analytical solutions to the system of equations for the ion sound and Langmuir waves. Phys Scr 2020;95(065602):1–10.